

UC Irvine

UC Irvine Previously Published Works

Title

Neuropathology of microbleeds in cerebral autosomal dominant arteriopathy with subcortical infarcts and leukoencephalopathy (CADASIL).

Permalink

<https://escholarship.org/uc/item/30r147j7>

Journal

Journal of Neuropathology and Experimental Neurology, 82(4)

Authors

Magaki, Shino

Chen, Zesheng

Severance, Alyscia

et al.

Publication Date


2023-03-20

DOI

10.1093/jnen/nlad004

Peer reviewed

Neuropathology of microbleeds in cerebral autosomal dominant arteriopathy with subcortical infarcts and leukoencephalopathy (CADASIL)

Shino Magaki , MD, PhD,^{1,*} Zesheng Chen, MD,^{1,†} Alyscia Severance, MD,¹ Christopher K. Williams,¹ Ramiro Diaz, BS,¹ Chuo Fang, MD, PhD,² Negar Khanlou, MD,¹ William H. Yong, MD,^{1,‡} Annlia Paganini-Hill, PhD,² Rajesh N. Kalaria, PhD, FRCPath,³ Harry V. Vinters, MD, FRCPC, FCAP,^{1,4,5} Mark Fisher, MD^{2,6}

¹Section of Neuropathology, Department of Pathology and Laboratory Medicine, Ronald Reagan UCLA Medical Center and David Geffen School of Medicine, Los Angeles, California, USA

²Department of Neurology, University of California-Irvine School of Medicine, Irvine, California, USA

³Translational and Clinical Research Institute, Newcastle University, Campus for Ageing and Vitality, Newcastle upon Tyne, UK

⁴Department of Neurology, Ronald Reagan UCLA Medical Center and David Geffen School of Medicine, Los Angeles, California, USA

⁵Brain Research Institute, Ronald Reagan UCLA Medical Center and David Geffen School of Medicine, Los Angeles, California, USA

⁶Department of Pathology and Laboratory Medicine, University of California-Irvine School of Medicine, Irvine, California, USA

[†]Present address: Centre Hospitalier Universitaire Sainte-Justine, Montréal, Quebec, Canada.

[‡]Present address: Department of Pathology and Laboratory Medicine, University of California-Irvine School of Medicine, Irvine, CA, USA.

Shino Magaki and Zesheng Chen contributed equally to this work.

*Send correspondence to: Shino Magaki, MD, PhD, Department of Pathology and Laboratory Medicine, Ronald Reagan UCLA Medical Center and David Geffen School of Medicine, Center for Health Sciences, Rm 1P-250, 10833 Le Conte Ave, Los Angeles, CA 90095-1732, USA; E-mail: smagaki@mednet.ucla.edu

ABSTRACT

Cerebral microbleeds (CMBs) detected on magnetic resonance imaging are common in patients with cerebral autosomal dominant arteriopathy with subcortical infarcts and leukoencephalopathy (CADASIL). The neuropathologic correlates of CMBs are unclear. In this study, we characterized findings relevant to CMBs in autopsy brain tissue of 8 patients with genetically confirmed CADASIL and 10 controls within the age range of the CADASIL patients by assessing the distribution and extent of hemosiderin/iron deposits including perivascular hemosiderin leakage (PVH), capillary hemosiderin deposits, and parenchymal iron deposits (PID) in the frontal cortex and white matter, basal ganglia and cerebellum. We also characterized infarcts, vessel wall thickening, and severity of vascular smooth muscle cell degeneration. CADASIL subjects had a significant increase in hemosiderin/iron deposits compared with controls. This increase was principally seen with PID. Hemosiderin/iron deposits were seen in the majority of CADASIL subjects in all brain areas. PVH was most pronounced in the frontal white matter and basal ganglia around small to medium sized arterioles, with no predilection for the vicinity of vessels with severe vascular changes or infarcts. CADASIL subjects have increased brain hemosiderin/iron deposits but these do not occur in a periarteriolar distribution. Pathogenesis of these lesions remains uncertain.

KEYWORDS: Aging, CADASIL, Cerebral microbleed, Hemosiderin, Immunohistochemistry, Small vessel disease

INTRODUCTION

Cerebral autosomal dominant arteriopathy with subcortical infarcts and leukoencephalopathy (CADASIL) is the most common heritable cause of stroke and vascular dementia (1, 2). It is caused by mutations in the *NOTCH3* gene at 19p13.1-13.2 encoding the Notch3 single transmembrane receptor that is expressed predominantly by vascular smooth muscle cells (VSMCs) and pericytes in adults (2–4). More than 230 different causal mutations, predominantly missense

mutations within the 23 exons (exons 2–24) encoding the 34 tandem epidermal growth factor-like (EGF-like) repeat sequences in the large Notch3 extracellular domain (N3ECD), have been reported (4–6).

CADASIL patients are characterized neuropathologically by multiple lacune-like infarcts predominantly in the subcortical white matter and deep gray matter and by diffuse white matter pallor (1, 4, 7–9). The pathologic changes in the vasculature in CADASIL patients mimic those of sporadic arteriolosclerosis

(1, 10). VSMC undergo degeneration, reflected by loss of α -smooth muscle actin (SMA) immunopositivity with hyalinization of affected vessel walls. On electron microscopy, granular osmiophilic (electron-dense) material (GOM) is seen in the inner media within the thickened basal lamina and closely juxtaposed to the VSMC plasma membrane or in the intercellular space (3, 4, 11). Immunogold labeling studies have found N3ECD to be localized in close proximity to and within GOMs (3, 12, 13).

The majority of CADASIL patients show white matter abnormalities on magnetic resonance imaging (MRI) (14). They also frequently demonstrate cerebral microbleeds (CMBs), a radiologic term used to describe small (<5–10 mm) well-defined round areas of signal void with associated “blooming” on paramagnetic-sensitive MRI sequences, such as T2*-weighted GRE and susceptibility-weighted imaging (SWI), in cortico-subcortical areas, deep gray matter, and the infratentorial compartment (15–17). However, CMBs are also associated with other conditions including sporadic and hereditary small vessel diseases (SVDs) such as cerebral amyloid angiopathy (CAA), and with hypertension, smoking, traumatic brain injury, and critical illness, and can even be seen in the general elderly population (18–21). CMBs have generally been associated with iron-containing deposits from blood or blood breakdown products, mainly hemosiderin. They are often found in the vicinity of vessels as perivascular hemosiderin deposits (PVH), thought to result from acute or chronic blood leakage/hemorrhage (15–17, 22–25). Other histopathologic findings associated with CMBs include vascular changes such as calcification/mineralization (26, 27), fibrinoid necrosis (24, 28), vessel wall dissection (29), microaneurysms (26, 29), vascular malformations including cavernous malformations (24, 30), and small cavities, some corresponding to lacunar infarcts on microscopic examination (29, 30).

After brain hemorrhage, the major breakdown products of hemoglobin are hemosiderin and hematoidin, which usually become visible 3–6 and 10–14 days after cerebral hemorrhage, respectively, although hemosiderin laden macrophages have been seen as early as 1–2 days in the skin and subcutaneous tissue after trauma (31–36). Macrophages/microglia can convert heme iron released from lysed red blood cells into iron-ferritin and then into hemosiderin, brown intra- and extracellular granules containing hydrous ferric oxide positive for Perls’ Prussian blue (PB) iron stain, which stains only nonheme iron, mostly in ferric form, such as in hemosiderin and ferritin (31, 32, 37–40). Further degradation of hemosiderin, especially in a low oxygen environment, results in opening of the porphyrin ring to form biliverdin (41). This is then reduced to form yellow hematoidin, chemically similar to bilirubin, which can be within histiocytes or extracellular, does not contain iron, and thus is not stained by PB stain (31, 32, 41, 42). Hemosiderin and hematoidin are poorly removed and can remain in situ indefinitely (31, 32).

The neuropathologic correlates, much less the pathogenic mechanism, of CMBs are unclear as few radiologic-pathologic correlative studies and even fewer pathologic studies focusing on hemosiderin/iron deposits including PVH, the likely histologic correlates of CMBs, have been conducted. In this retrospective autopsy study, we characterized hemosiderin/iron

deposits in various compartments of the brain and their associations with the degree and distribution of vascular changes and ischemic lesions in CADASIL patients and controls.

MATERIALS AND METHODS

Subjects

Postmortem brain tissue from the frontal lobe, basal ganglia, and cerebellum from 10 patients with genetically confirmed CADASIL, previously described in Hase et al (43) and Yamamoto et al (44), were obtained from Newcastle University, UK, as 10- μ m-thick paraffin sections on large microscope slides (50 \times 75 mm), medium-sized microscope slides (40 \times 75 mm), and standard microscope slides (25 \times 75 mm), except for one CADASIL case (CAD1) in which only 5- μ m-thick sections were available. Two cases were excluded from analysis for prolonged formalin fixation time of >20 years. These brain regions were chosen based on the known involvement of the frontal white matter and basal ganglia with lesser involvement of the cerebellum (8), and on availability of tissue. They were sampled using the standard protocol of the Newcastle Brain Tissue Resource. We also examined paraffin sections cut at 10 μ m on standard microscope slides from the same regions from 10 controls, within the age range of the CADASIL patients, who underwent autopsies for non-neurologic diseases at UCLA Medical Center, Los Angeles, CA, between 2013 and 2019 (inclusive) and showed no significant cerebrovascular or neurodegenerative disease. Written informed consent was obtained from all subjects included in the study.

Histopathologic assessment for vascular disease, hemosiderin/hematoidin, and Prussian blue-positive deposits

Sections were stained with hematoxylin and eosin (H&E) and PB iron stain. PB staining was performed using the EpreDia Iron Stain kit (Kalamazoo, MI). Sections were incubated with a 1:1 solution of potassium ferrocyanide and 20% hydrochloric acid for 30 minutes at room temperature, rinsed with deionized water, counterstained with a nuclear red thiazin stain solution for 45 seconds, and then rinsed with deionized water again.

H&E sections were assessed for infarcts and arteriolosclerosis according to the VCING guidelines (45, 46) except in vessels less than 300 μ m in diameter, although there is no consensus definition of an arteriole based on lumen size (47, 48). Infarcts were classified as cystic or macroinfarcts (\geq 1 cm), lacunar infarcts (grossly visible but <1 cm), and microinfarcts (not visible grossly but detected on microscopic examination). Arteriolo-sclerosis was graded on a 0–3 scale: 0 = normal, 1 = mild fibrosis with mild medial thickening, 2 = moderate fibrosis, and 3 = severe fibrosis, based on overall impression (45, 46).

We characterized the various findings related to hemosiderin deposits and PB-positive iron deposits in our CADASIL and control subjects. Hemorrhage was classified as large hemorrhage (visible grossly) or microhemorrhage (seen only on microscopic examination) and defined by the accumulation of hemosiderin in the brain parenchyma, according to the

VCING guidelines (45). Histopathology does not allow for a distinction between hemorrhagic infarct and hemorrhage or between microinfarcts and microhemorrhages in which the blood has been cleared (49). In this study, if the lesion predominantly appeared as an infarct/microinfarct but with focal hemosiderin laden macrophages/hemosiderin deposits, it was categorized as a hemorrhagic infarct/microinfarct.

Perivascular hemosiderin/hematoidin leakage (PVH) was defined as hemosiderin granule deposits in the perivascular space, predominantly arterioles but also venules, with specific inclusion of hematoidin and exclusion of capillaries (45, 46). Perivascular hemosiderin/hematoidin leakage in each region was scored according to the VCING criteria on a 0–3 scale as: 0 = 0, 1 = <3, 2 = 3–5, and 3 = >5 hemosiderin granule deposits, based on the most severe lesion (45, 46, 50). Additionally, the number of foci/blood vessels with PVH was counted in 10 contiguous fields at 200× magnification to determine the density of PVH.

PB positive granules associated with capillaries were designated as capillary hemosiderin deposits (CHDs). PB positive granules in the parenchyma not associated with vessels (arterioles, venules, or capillaries) were designated as parenchymal iron deposits (PIDs) with the caveat that the iron deposits in the basal ganglia may not be reflective of hemorrhage but of increased iron in the region (32, 51–53). Similar to PVH, the foci of CHD and PID were counted in 10 contiguous fields at 200× magnification to assess the density of deposits per field (54).

Immunohistochemistry for α -SMA and β -amyloid 1–40

Sections were incubated with primary antibody to α -SMA (prediluted, mouse monoclonal, 1A4; Cell Marque, Rocklin, CA) followed by horse antimouse secondary antibody conjugated to horseradish peroxidase (MP7402; Vector Laboratories, Burlingame, CA). Antibody reactivity was visualized with NovaRED substrate kit (no. SK-4800; Vector Laboratories) and counterstained with hematoxylin. Loss of SMA staining was graded on a 0–3 scale as: 0 = none to minimal loss, 1 = \leq 50% loss, 2 = >50% loss, 3 = complete or nearly complete loss, based on overall impression (Fig. 1). As CAA is associated with CMBs, its presence was assessed in the frontal lobe by β -amyloid 1–40 immunohistochemistry (1:400, rabbit polyclonal, AB5074P; EMD Millipore, Burlington, MA) followed by horse antirabbit antibody conjugated to horseradish peroxidase (MP7402; Vector Laboratories). Antibody reactivity was visualized with diaminobenzidine as chromogen (no. SK-4100; Vector Laboratories) and counterstained with hematoxylin.

Statistical analysis

The densities of foci of PVH, CHD, and PID were compared between CADASIL and control patients using the nonparametric Mann-Whitney U test and between different regions using the Kruskal-Wallis test with Dunn's correction for multiple comparisons. Group comparisons between absent/minimal-mild and moderate-severe (score \geq 2) degrees of arteriolosclerosis, PVH, and SMA loss were performed with the Fisher exact test. A p value <0.05 was considered statistically significant.

RESULTS

Demographic and clinical data

The demographic and clinical characteristics of the 8 CADASIL patients and 10 controls are summarized in Table 1. The CADASIL patients had an average age of 57.5 ± 8.2 (standard deviation [SD]) with a range of 44–68 years. There were 5 males and 3 females. All had some degree of cognitive impairment, 5 severe and 3 mild. Two had a history of smoking. The controls had an average age of 57.6 ± 7.1 (SD) with a range of 47–68 years and included 5 males and 5 females. One control had a history of smoking and 3 had a history of hypertension. Detailed clinical history was unavailable in 2 controls transferred for autopsy from outside hospitals. Only limited MRI findings (without details on CMBs) were available, but the majority of CADASIL subjects demonstrated extensive white matter hyperintensities and multiple lacunar infarcts.

Pathologic findings

No grossly visible hemorrhages were seen in the brains of the CADASIL patients although infarct/microinfarcts with focal hemosiderin laden macrophages (hemorrhagic infarct/microinfarcts) were present on histopathologic examination in three (Table 2). One control demonstrated a microhemorrhage in the frontal white matter but no large hemorrhages. Characteristically, all CADASIL subjects showed at least one infarct in the frontal lobe, basal ganglia, or cerebellum, although many demonstrated multiple infarcts, most frequently in the basal ganglia (Fig. 2). The degree of arteriolosclerosis and loss of SMA staining were also high in the majority of CADASIL subjects, not only in the frontal white matter and basal ganglia but also the cerebellar white matter. Arteriolosclerosis was absent to mild in all controls in the frontal cortex and cerebellar white matter and in the majority of controls in the frontal white matter and basal ganglia; none showed more than minimal SMA loss. As expected, the proportion of CADASIL subjects with moderate to severe arteriolosclerosis (score \geq 2) as well as with SMA loss in all regions except the frontal cortex was greater than that of controls (Table 2) ($p < 0.01$). None of the CADASIL or control subjects showed CAA on β -amyloid 1–40 immunostain although one CADASIL subject showed scattered diffuse plaques, one control subject scattered cored and diffuse plaques, one control subject scattered diffuse plaques, and one control subject rare diffuse plaques.

PVH were frequently seen in all regions in both CADASIL and control subjects. One or more foci of perivascular hemosiderin/hematoidin leakage, mainly around small to medium sized arterioles, was seen in the frontal white matter and basal ganglia in all subjects (Fig. 2). All foci of PVH comprised small clusters of hemosiderin/hematoidin deposits without expansion of the perivascular space and were seen around both arteriolosclerotic and nonarteriolosclerotic vessels. In both groups, the density of PVH was significantly higher in the frontal and cerebellar white matter compared to the frontal cortex. In CADASIL subjects, the density of PVH was also significantly higher in the basal ganglia compared to frontal cortex. However, CADASIL subjects did not differ from controls in proportion of moderate to severe (score \geq 2) PVH. Furthermore,

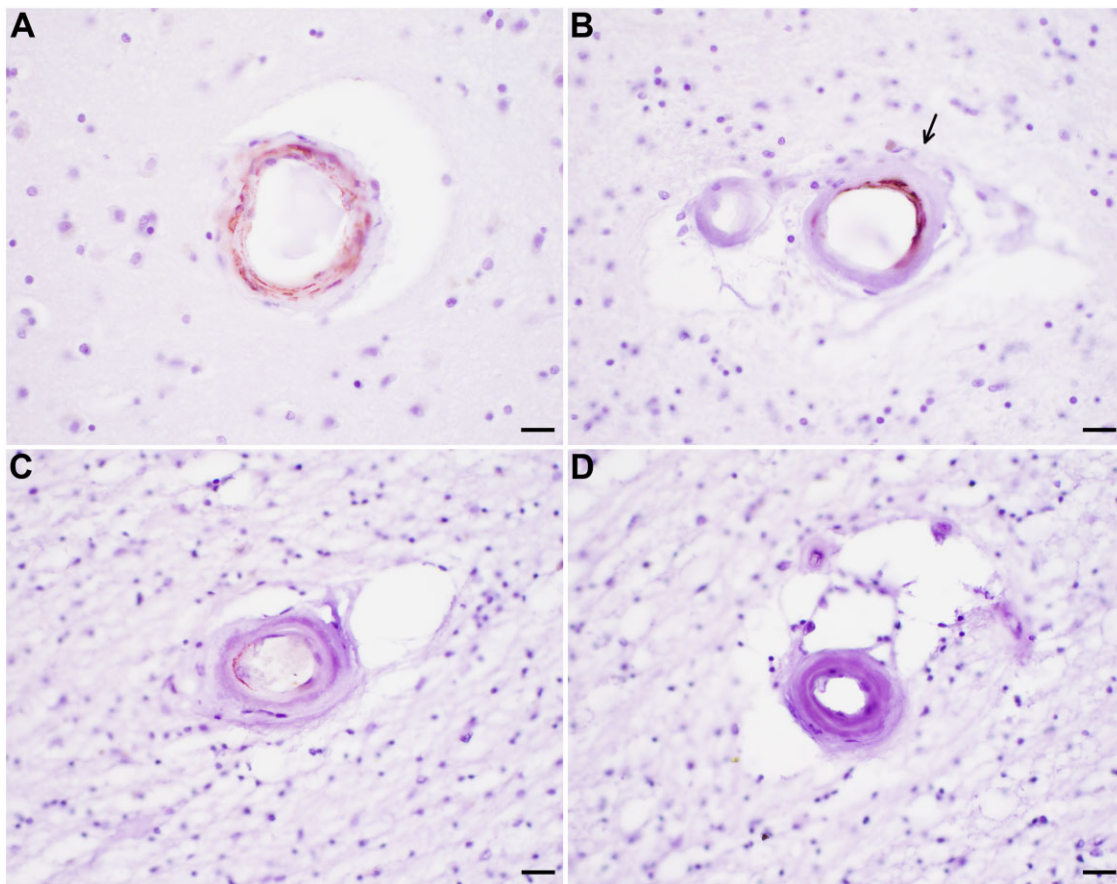


Figure 1. Grading of α -smooth muscle actin (SMA) loss on immunohistochemistry. (A) 0 = none to minimal loss of SMA staining, (B) 1 = $\leq 50\%$ loss of SMA staining (arrow), (C) 2 = $>50\%$ loss of SMA staining, (D) 3 = complete or nearly complete loss of SMA staining in vessel walls. Scale bars: A–D = 20 μm .

severity (score <2 vs ≥ 2) of PVH did not differ with arteriosclerosis or SMA loss in any of the regions examined in CADASIL subjects and controls.

CADASIL subjects showed significantly increased hemosiderin/iron deposition of all categories compared with controls for all regions combined (Fig. 3A, $p = 0.04$). When broken down by category, PID, but not PVH and CHD, was significantly increased in the CADASIL subjects for all brain regions combined (Fig. 3B, $p < 0.05$). As shown before by Fisher et al (55), some of the iron associated with capillaries appeared to localize within pericytes (Fig. 4A), while what appeared to be extracellular hemosiderin granules adjacent to capillaries highlighted by PB stain were also seen (Fig. 4C, D). In both CADASIL and control groups, CHD density in the basal ganglia was higher than in all other regions. The density of PID was also highest in the basal ganglia (Fig. 3C) followed by the cerebellar white matter (Fig. 3F), and significantly higher in both regions compared to the frontal cortex (Fig. 3D) and white matter (Fig. 3E) in CADASIL subjects. Similar findings were seen in controls with significantly higher density of PID in the basal ganglia compared to frontal cortex and white matter and cerebellar white matter. At least some of these PID appeared to correspond to small parenchymal hemosiderin deposits on H&E (Fig. 4B–D). Although PID were defined as deposits that did not appear to be associated with capillaries, it

is possible some may in fact had been associated with capillaries out of the plane of section and therefore should really be categorized as CHD. The density of PID was significantly higher in the frontal and cerebellar white matter in CADASIL subjects compared with controls (Fig. 3, $p < 0.05$ and $p < 0.01$, respectively), which remained significant for the combined density of PID and CHD. The CADASIL and control groups did not differ in density of PID in the frontal cortex, which showed very few PID in both groups, or in the basal ganglia, which showed the highest density of PID in both groups. None of the different types of hemosiderin/hematoïdin or PB positive deposits showed a predilection for the vicinity of infarcts or vessels with arteriosclerosis. A few CADASIL and control subjects demonstrated microvascular mineralization, occasionally shown to correspond to CMBs on MRI (26, 27), in the basal ganglia with positivity for PB (Fig. 4E, F).

DISCUSSION

The majority of CMBs have been thought to correspond to blood or blood breakdown products such as hemosiderin, especially PVH. However, PVH is commonly seen in brain autopsies in patients with no known neurologic disease. To help bridge the “disconnect” between imaging features and

Table 1. Demographic and clinical data of CADASIL and age-matched control subjects

Case/cohort (n)	Age (\pm SD)	Sex	Mutation	Disease duration	Clinical features	MRI findings
CAD1	61	M	Arg169Cys	10	Severe vascular cognitive impairment, obesity	Confluent WMHs, lacunar infarcts in basal ganglia and brainstem
CAD2	53	F	Arg133Cys	6	Mild vascular cognitive impairment	Nodular periventricular WMHs
CAD3	55	M	Arg558Cys	11	Mild vascular cognitive impairment	Confluent periventricular and deep WMHs, lacunar infarcts in brainstem
CAD4	68	F	Arg133Cys	18	Severe vascular cognitive impairment, history of smoking	Confluent WMHs, lacunar infarcts in basal ganglia and brainstem
CAD5	52	M	Arg141Cys	10	Severe vascular cognitive impairment	Confluent WMHs, lacunar infarcts in basal ganglia and brainstem
CAD6	59	M	Arg169Cys	12	Severe vascular cognitive impairment	Confluent WMHs, lacunar infarcts in basal ganglia and brainstem
CAD7	44	F	Arg153Cys	8	Mild vascular cognitive impairment, diabetes	Confluent WMHs, lacunar infarcts in basal ganglia
CAD8	68	M	Arg153Cys	28	Severe vascular cognitive impairment, history of smoking	Not available
CADASIL cases (8)	57.5 \pm 8.2	5 M/3 F	—	—		
Controls (10)	57.6 \pm 7.1	5 M/5 F	N/A	N/A	1 subject with history of smoking, 3 with hypertension	N/A

M, male; F, female; N/A, not applicable; SD, standard deviation; WMHs, white matter hyperintensities.

autopsy findings, we conducted a neuropathologic autopsy study examining CADASIL patients, who have pronounced vascular changes in the brain and are a model of inherited SVD (56, 57). We assessed whether hemosiderin/iron, the histologic correlate of CMBs, is increased pathologically in CADASIL patients. This has implications for other conditions, such as CAA and hypertension, which are also associated with CMBs. We found significantly increased hemosiderin/iron deposits in CADASIL subjects compared with controls. While both CADASIL and control subjects had hemosiderin deposits associated with capillaries and larger vessels, the increase in hemosiderin/iron in CADASIL was not associated with obvious elements of the brain vasculature. CADASIL subjects also had significantly increased arteriolosclerosis with SMA loss; however, these vascular changes did not correspond to increased hemosiderin/iron deposition.

The increased PID in the frontal and cerebellar white matter of CADASIL subjects may originate from capillary leakage/blood-brain barrier (BBB) disruption. No difference in CHD was seen between CADASIL and control subjects. However, capillaries may have been out of the plane of section or destroyed by the hemorrhage as reduced capillary density in white matter lesions and around lacunar infarcts as well as degenerating capillaries have been seen in CADASIL subjects (56, 58). Although disruption of the BBB has not been associated with PB positivity in a cohort of elderly individuals including those with neurodegenerative disease (59) or in CADASIL subjects with white matter lesions (56), we could be examining

only the sequelae of BBB injury or injury at a different site (59). BBB disruption has been associated with CMBs in a mouse model of inflammation-induced CMBs (60) as well as with regional iron burden on imaging in CADASIL (57). Furthermore, pericytes, key components of the BBB or neurovascular unit, postulated to phagocytose erythrocytes that pass through the BBB with macrophages (55), have been shown to be decreased in a mouse model of CADASIL (61). This was not observed in CADASIL subjects and requires further investigation (56, 62). Brain hemosiderin may also be a marker for ischemia and alterations in iron metabolism and clearance (52, 63). In the brain, oligodendrocytes are the major reservoir of iron and iron-binding proteins, including the iron storage protein ferritin and the iron transport protein transferrin, needed for myelination (64, 65). Oligodendrocyte vulnerability to ischemia during development underlies perinatal white matter injury and such susceptibility may also play a role in white matter diseases such as multiple sclerosis (MS) (52, 66–68).

In CADASIL patients, cognitive impairment is seen even before the occurrence of transient ischemic attack/stroke (69), with early decreased cerebral blood flow in the white matter associated with T2 weighted white matter changes on MRI (70). White matter axonal abnormalities correlate with SVD, and are especially pronounced in CADASIL and particularly in the frontal lobe white matter (71). This suggests that the vascular changes that lead to cerebral hypoperfusion and a chronic hypoxic state in the deep white matter may result in loss of myelination, a mechanism that has also been implicated

Table 2. Pathologic findings in CADASIL and age-matched control subjects

Frontal lobe cortex	Microinfarcts	Lacunar infarcts	Large infarcts	Arteriolosclerosis score*	SMA loss score	PVH leakage score*
CAD1	0	0	0	2	0	2
CAD2	0	0	0	1	1	0
CAD3	4	2 [†]	0	1	0	3
CAD4	0	0	0	1	0	1
CAD5	0	0	0	1	N/A	1
CAD6	0	0	0	2	1	1
CAD7	0	0	0	1	0	1
CAD8	1	0	0	2	0	0
CADASIL						
Score ≥2 (%)				3 (38%)	0 (0%)	2 (25%)
Score <2 (%)				5 (63%)	7 (100%)	6 (75%)
Controls [†]						
Score ≥2 (%)				0 (0%)	0 (0%)	2 (25%)
Score <2 (%)				8 (100%)	8 (100%)	6 (75%)
Frontal lobe white matter	Microinfarcts	Lacunar infarcts	Large infarcts	Arteriolosclerosis score*	SMA loss score	PVH leakage score*
CAD1	0	0	0	3	1	2
CAD2	0	0	0	2	1	3
CAD3	0	0	1 [†]	2	2	3
CAD4	0	0	0	3	2	2
CAD5	0	0	0	3	N/A	3
CAD6	2	0	0	3	2	1
CAD7	1	4	0	3	2	3
CAD8	0	1	0	3	2	3
CADASIL						
Score ≥2 (%)				8 (100%) [§]	5 (71%) [§]	7 (88%)
Score <2 (%)				0 (0%)	2 (29%)	1 (13%)
Controls						
Score ≥2 (%)				1 (13%)	0 (0%)	8 (100%)
Score <2 (%)				7 (88%)	8 (100%)	0 (0%)
Basal ganglia	Microinfarcts	Lacunar infarcts	Large infarcts	Arteriolosclerosis score*	SMA loss score	PVH leakage score*
CAD1	2	0	0	3	1	1
CAD2	2 [†]	0	0	2	2	3
CAD3	2	0	1	3	2	3
CAD4	0	0	0	3	1	3
CAD5	2 [†]	0	0	3	N/A	1
CAD6	1	2	0	3	2	2
CAD7	1	0	0	2	2	3
CAD8	1	1	0	3	2	1
CADASIL						
Score ≥2 (%)				8 (100%) [§]	5 (71%) [§]	5 (63%)
Score <2 (%)				0 (0%)	2 (29%)	3 (38%)
Controls						
Score ≥2 (%)				3 (30%)	0 (0%)	7 (70%)
Score <2 (%)				7 (70%)	10 (100%)	3 (30%)
Cerebellar white matter	Microinfarcts	Lacunar infarcts	Large infarcts	Arteriolosclerosis score*	SMA loss score	PVH leakage score*
CAD1	0	0	0	3	0	0
CAD2	0	0	0	3	2	2
CAD3	0	0	0	1	0	3
CAD4	1	0	0	3	2	1
CAD5	0	0	0	3	N/A	3
CAD6	N/A	N/A	N/A	N/A	N/A	N/A
CAD7	1	1	0	2	2	3
CAD8	2	0	0	3	2	3
CADASIL						
Score ≥2 (%)				6 (86%) [§]	4 (67%) [§]	5 (71%)
Score <2 (%)				1 (14%)	2 (33%)	2 (29%)
Controls						
Score ≥2 (%)				0 (0%)	0 (0%)	7 (70%)
Score <2 (%)				10 (100%)	10 (100%)	3 (30%)

N/A, not available; PVH, perivascular hemosiderin.

* According to VCING criteria (Skrobot et al [45]).

† Focal hemosiderin deposits/Prussian blue positivity.

‡ No infarcts in any of the regions were seen in control patients.

§ CADASIL vs controls, $p < 0.01$ by Fisher exact test.

|| One control patient demonstrated a microhemorrhage in the frontal white matter which was not included.

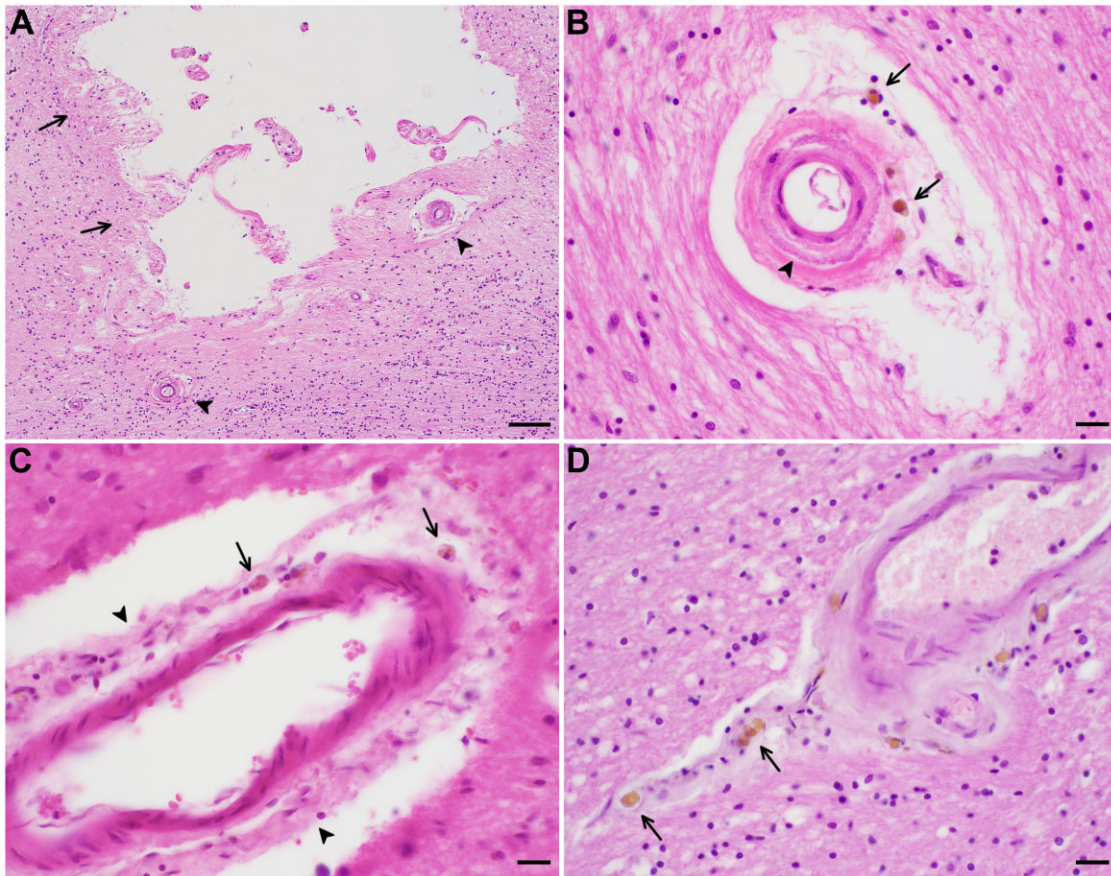


Figure 2. (A) Lacunar infarct in the frontal lobe white matter (arrows) with surrounding round thick-walled vessels (arrowheads) in a CADASIL patient (CAD7). (B) Magnified view of vessel in frontal white matter with marked thickening of the wall and basophilic granular material in the tunica media (arrowhead) with perivascular hemosiderin deposits (arrows). (C) Moderate arteriolosclerosis with adventitial fibrosis (arrowheads) and perivascular fine hemosiderin deposits within macrophages (arrows) in the basal ganglia of a control patient. (D) Vessel with moderate arteriolosclerosis and many perivascular hematoidin deposits (arrows) in the frontal white matter of a different control patient. Scale bars: A = 100 μm ; B–D = 20 μm .

in MS (58, 67, 71). Rajani et al (56) demonstrated that in CADASIL patients, BBB disruption was seen in white matter pallor that was associated with lacunes or enlarged perivascular spaces (ePVs) but not in white matter pallor not associated with lacunes or ePVs (“pure” white matter lesions), suggesting that other mechanisms such as hypoxia may have a greater role in the development of these “pure” white matter lesions. Thus, in addition to an interaction of multiple factors, regional effects such as proximity to another lesion or downstream of vascular changes may play a part. Furthermore, a subset of CD163-positive perivascular macrophages has been associated with hemosiderin deposition (52). This has been postulated to represent an attempt at clearance via macrophages of brain iron released from oligodendrocytes in the setting of ischemic damage, since there is no known export pathway for iron from the brain (52). It could also be in response to erythrocyte leakage (52). Thus, the hemosiderin/iron observed could be the result of both erythrocyte leakage and release of iron from oligodendrocytes in ischemia. Strassman (32) observed that hemosiderin after hemorrhage has similar microscopic features and staining pattern as iron in areas of the brain with no evidence of prior hemorrhage or thrombosis, except for histiocytes with

fine hemosiderin granules in areas of old hemorrhage and thrombosis. Such macrophages containing fine hemosiderin granules were only found in the microhemorrhage in one control, focally in the infarcts in the CADASIL subjects, and in a subset of PVH foci (Fig. 2C) in both groups.

The increase in PID was not seen in the frontal cortex, which is relatively less affected compared to the frontal subcortical white matter, in CADASIL. Interestingly, the basal ganglia showed no significantly increased PID or other types of hemosiderin/iron deposits compared with controls despite being severely affected in CADASIL. Both CADASIL and control patients showed mildly increased PB staining in the dentate nucleus of the cerebellum and had diffuse and pale, nongranular PB staining in the basal ganglia, especially in the striatopallidal fibers (pencils of Wilson) likely due to staining for ferritin (Fig. 4B). This is consistent with known high iron content in the basal ganglia and cerebellar dentate nucleus (32, 39, 53, 72). Ferritin cannot be seen on H&E, but PB stain highlights both hemosiderin and ferritin, with ferritin showing pale diffuse staining while hemosiderin stains as coarse granules (40, 72). Imaging studies have shown increased iron content in the deep gray matter in CADASIL patients compared

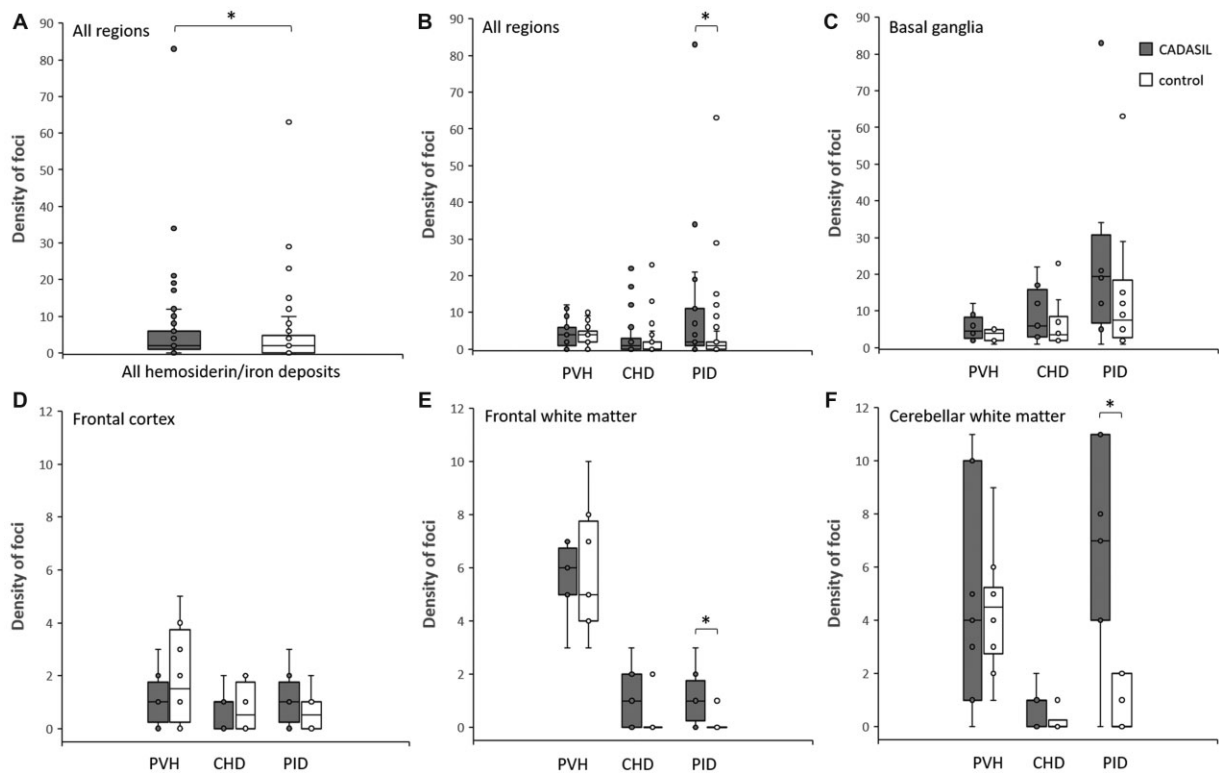


Figure 3. Box and whisker plots (showing median, interquartile range, and full range) of density (foci per ten 200 \times fields) of (A) all types of hemisiderin/iron deposits in all regions combined in CADASIL and control patients, and perivascular hemisiderin/hematoidin leakage (PVH), capillary hemisiderin deposits (CHDs), and parenchymal iron deposits (PIDs) in (B) all regions combined, (C) basal ganglia, (D) frontal cortex, (E) frontal white matter, and (F) cerebellar white matter in CADASIL and control patients, * $p < 0.05$.

with controls (73, 74). CMB assessment by MRI of basal ganglia can be unreliable, however, due to false positive signals from high iron content and frequent microvascular calcification/mineralization in the region, especially in MRI studies using high magnetic field strengths or SWI (16, 75–77). PB can stain microvascular calcification or, more accurately, mineralization as other minerals including iron are consistently detected in these vessel walls and calcium rarely (76–79). Thus, use of the PB stain without concomitant evaluation on H&E may result in false positives, but mineralization can be easily differentiated from hemisiderin deposits on H&E stain (78, 79). It is possible that no difference was seen in hemisiderin/iron deposits in the basal ganglia between CADASIL and control subjects due to the high baseline levels of iron in that region with subtle differences not readily detectable on histology. Although thickened arterioles and frequent infarcts in the cerebral white matter and basal ganglia are hallmark features of CADASIL, arterioles in the cerebral white matter are stenotic while those in the basal ganglia are not, suggesting a differing pathogenesis of ischemia in these two regions, of stenosis and hemodynamic disturbances, respectively (9).

PVH was frequent in all brain regions in both our CADASIL and control subjects, consistent with previous histologic studies in which PVH was found to be common in all age groups in many regions (50, 52). Janaway et al (52) found that 99% of brains from individuals aged 65 years and over showed hemisiderin deposition, perivascular and/or in neuropil, in the putamen. Dallaire-Th eroux et al also showed that in their cohort of cognitively healthy adults aged 19–84 years the majority showed PVH, as defined by the VCING criteria (45, 50). CMBs in the general elderly population are detected in approximately 18% of individuals in their 60s to over 35% in those over 80 years of age (21) while 30%–70% of CADASIL patients demonstrate CMBs on MRI (22, 23, 80–83), consistent with a much higher sensitivity of histologic examination in detecting PVH compared to imaging (27, 84). CMB prevalence also increases with age in CADASIL patients (83). PVH may be a marker for fragility of vessels in dementia and old age (46, 50, 85). As CMBs, presumed to correspond to PVH, are thought to result from structural changes in the vessels, it is intriguing that we saw no increase in PVH in CADASIL patients where the vascular alterations, with arteriolosclerosis and degeneration of the tunica media and loss of SMA staining, are exceptionally severe. Although our controls are from hospital-based autopsies and are not reflective of the general population, the similar prevalence and severity of PVH in our CADASIL and control groups suggest that the vascular changes characteristic of CADASIL may not necessarily lead to increased vascular fragility at least at the level of the arterioles/arteries.

Our study has several limitations. We did not have detailed MRI data, specifically regarding CMBs, on the subjects. Another limitation is the small number of CADASIL cases

with controls (73, 74). CMB assessment by MRI of basal ganglia can be unreliable, however, due to false positive signals from high iron content and frequent microvascular calcification/mineralization in the region, especially in MRI studies using high magnetic field strengths or SWI (16, 75–77). PB can stain microvascular calcification or, more accurately, mineralization as other minerals including iron are consistently detected in these vessel walls and calcium rarely (76–79). Thus, use of the PB stain without concomitant evaluation on H&E may result in false positives, but mineralization can be easily differentiated from hemisiderin deposits on H&E stain (78, 79). It is possible that no difference was seen in hemisiderin/iron deposits in the basal ganglia between CADASIL and control subjects due to the high baseline levels of iron in that region with subtle differences not readily detectable on histology. Although thickened arterioles and frequent infarcts in the cerebral white matter and basal ganglia are hallmark features of CADASIL, arterioles in the cerebral white matter are stenotic while those in the basal ganglia are not, suggesting a differing pathogenesis of ischemia in these two regions, of stenosis and hemodynamic disturbances, respectively (9).

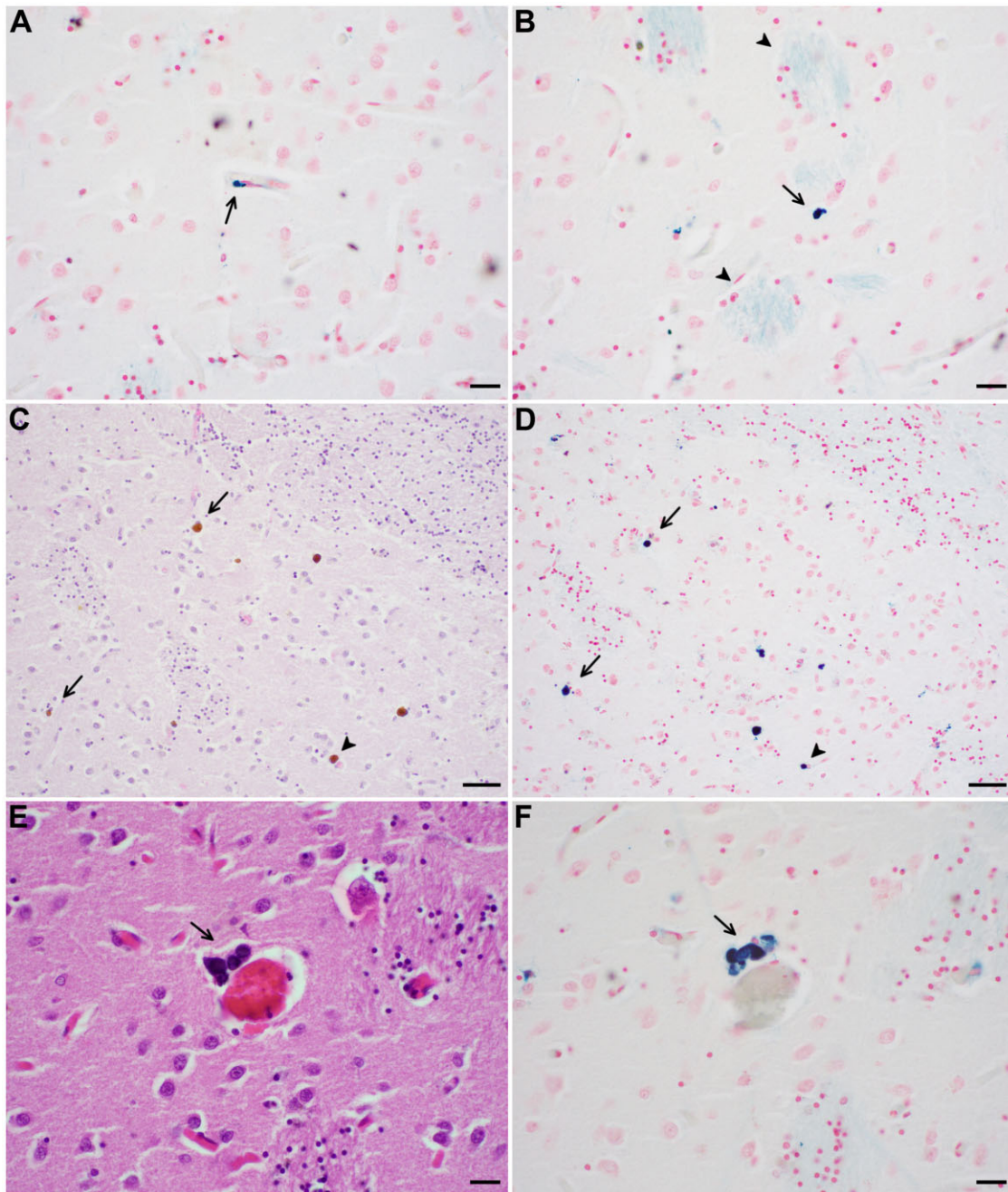


Figure 4. (A) Capillary hemosiderin deposit (CHD, arrow) in the basal ganglia and (B) Prussian blue (PB)-positive deposit (PID, arrow) in the parenchyma of the basal ganglia in a CADASIL subject. The striatopallidal fibers (arrowheads) show pale diffuse PB staining. (C) Scattered hemosiderin/iron deposits associated with a capillary (CHD, arrowhead) and in the parenchyma (PID, arrows) on H&E stain (D) with same region on PB stain highlighting the hemosiderin/iron deposits (CHD, arrowhead; PID, arrows). (E) Perivascular mineralization (arrow) (F) also positive for PB. Scale bars: A, B = 20 μm ; C, D = 50 μm ; E, F = 20 μm .

with a mix of mutations available for examination. Furthermore, although our controls did not have significant cerebrovascular or neurodegenerative disease, they were from hospital-based autopsy cases (and from a different hospital in a different country) and thus many had clinical risk factors for CMBs such as critical illness and hypertension (19). Finally, the distinction between CHD and PID was dependent on detecting a capillary associated with the deposit. As capillaries are approximately 3–10 μm in diameter (47), some capillaries

may have been out of the plane of section, leading to miscategorization of CHD as PID.

In summary, these findings suggest complex factors, including capillary leakage and white matter ischemia, underlying hemosiderin deposition in the brains of CADASIL patients. The characteristic vascular changes in CADASIL may initiate downstream effects resulting in increased PID possibly through capillary leakage with BBB disruption and/or ischemic changes. This may lead to iron dysregulation with white matter

damage and myelin loss that contribute to early cognitive dysfunction and manifest as hemosiderin/iron deposits in the brain in later stages. Leakage at the site of vascular thickening and degeneration, manifesting as PVH, remains a possibility although severity of PVH was not associated with local vascular changes in our study. It is important to understand the pathologic substrate of CMBs and mechanism of hemosiderin/iron deposition, not only for CADASIL but for other diseases associated with CMBs, as CMBs are associated not only with increased risk for ischemic infarcts and intracerebral hemorrhage but also with death and dementia (17).

FUNDING

HVV and SM are supported in part by the Mary S. Easton Center for Alzheimer's Research and Care at University of California Los Angeles. MF is supported in part by National Institutes of Health R01 NS020989.

CONFLICT OF INTEREST

The authors have no duality or conflicts of interest to declare.

REFERENCES

- Vinters HV, Zarow C, Borys E, et al. Review: Vascular dementia: Clinicopathologic and genetic considerations. *Neuropathol Appl Neurobiol* 2018;44:247–66
- Joutel A, Corpechot C, Ducros A, et al. Notch3 mutations in CADASIL, a hereditary adult-onset condition causing stroke and dementia. *Nature* 1996;383:707–10
- Joutel A, Andreux F, Gaulis S, et al. The ectodomain of the Notch3 receptor accumulates within the cerebrovasculature of CADASIL patients. *J Clin Invest* 2000;105:597–605
- Tikka S, Baumann M, Siitonen M, et al. CADASIL and CARASIL. *Brain Pathol* 2014;24:525–44
- Joutel A, Favrole P, Labauge P, et al. Skin biopsy immunostaining with a Notch3 monoclonal antibody for CADASIL diagnosis. *Lancet* 2001;358:2049–51
- Xiromerisiou G, Marogianni C, Dadouli K, et al. Cerebral autosomal dominant arteriopathy with subcortical infarcts and leukoencephalopathy revisited: Genotype-phenotype correlations of all published cases. *Neurol Genet* 2020;6:e434
- Ruchoux MM, Maurage CA. CADASIL: Cerebral autosomal dominant arteriopathy with subcortical infarcts and leukoencephalopathy. *J Neuropathol Exp Neurol* 1997;56:947–64
- Chabriat H, Vahedi K, Iba-Zizen MT, et al. Clinical spectrum of CADASIL: A study of 7 families. *Lancet* 1995;346:934–9
- Miao Q, Paloneva T, Tuisku S, et al. Arterioles of the lenticular nucleus in CADASIL. *Stroke* 2006;37:2242–7
- Yamamoto Y, Craggs LJJ, Watanabe A, et al. Brain microvascular accumulation and distribution of the NOTCH3 ectodomain and granular osmiophilic material in CADASIL. *J Neuropathol Exp Neurol* 2013;72:416–31
- Baudrimont M, Dubas F, Joutel A, et al. Autosomal dominant leukoencephalopathy and subcortical ischemic stroke. *Stroke* 1993;24:122–5
- Ishiko A, Shimizu A, Nagata E, et al. Notch3 ectodomain is a major component of granular osmiophilic material (GOM) in CADASIL. *Acta Neuropathol* 2006;112:333–9
- Monet-Leprêtre M, Haddad I, Baron-Menguy C, et al. Abnormal recruitment of extracellular matrix proteins by excess Notch3 ECD: A new pathomechanism in CADASIL. *Brain* 2013;136:1830–45
- Salamon N. Neuroimaging of cerebral small vessel disease. *Brain Pathol* 2014;24:519–24
- Martinez-Ramirez S, Greenberg SM, Viswanathan A. Cerebral microbleeds: Overview and implications in cognitive impairment. *Alzheimers Res Ther* 2014;6:33
- Greenberg SM, Vernooij MW, Cordonnier C, et al.; Microbleed Study Group. Cerebral microbleeds: A guide to detection and interpretation. *Lancet Neurol* 2009;8:165–74
- Charidimou A, Shams S, Romero JR, et al.; International META-MICROBLEEDS Initiative. Clinical significance of cerebral microbleeds on MRI: A comprehensive meta-analysis of risk of intracerebral hemorrhage, ischemic stroke, mortality, and dementia in cohort studies (v1). *Int J Stroke* 2018;13:454–68
- Puy L, Pasi M, Rodrigues M, et al. Cerebral microbleeds: From depiction to interpretation. *J Neurol Neurosurg Psychiatry* 2021;92:598–607
- Fanou EM, Coutinho JM, Shannon P, et al. Critical illness-associated cerebral microbleeds. *Stroke* 2017;48:1085–7
- Agarwal S, Jain R, Dogra S, et al. Cerebral microbleeds and leukoencephalopathy in critically ill patients with COVID-19. *Stroke* 2020;51:2649–55
- Vernooij MW, van der Lugt A, Ikram MA, et al. Prevalence and risk factors of cerebral microbleeds: The Rotterdam scan study. *Neurology* 2008;70:1208–14
- Oberstein SAJL, van den Boom R, van Buchem MA, et al.; Dutch CADASIL Research Group. Cerebral microbleeds in CADASIL. *Neurology* 2001;57:1066–70
- Dichgans M, Holtmannspötter M, Herzog J, et al. Cerebral microbleeds in CADASIL: A gradient-echo magnetic resonance imaging and autopsy study. *Stroke* 2002;33:67–71
- van Veluw SJ, Biessels GJ, Klijn CJM, et al. Heterogeneous histopathology of cortical microbleeds in cerebral amyloid angiopathy. *Neurology* 2016;86:867–71
- Shoamanesh A, Kwok CS, Benavente O. Cerebral microbleeds: Histopathological correlation of neuroimaging. *Cerebrovasc Dis* 2011;32:528–34
- Tatsumi S, Shinohara M, Yamamoto T. Direct comparison of histology of microbleeds with postmortem MR images: A case report. *Cerebrovasc Dis* 2008;26:142–6
- Haller S, Montandon ML, Lazeyras F, et al. Radiologic-histopathologic correlation of cerebral microbleeds using pre-mortem and post-mortem MRI. *PLoS One* 2016;11:e0167743
- van Veluw SJ, Scherlek AA, Freeze WM, et al. Different microvascular alterations underlie microbleeds and microinfarcts. *Ann Neurol* 2019;86:279–92
- Schrag M, McAuley G, Pomakian J, et al. Correlation of hypointensities in susceptibility-weighted images to tissue histology in dementia patients with cerebral amyloid angiopathy: A postmortem MRI study. *Acta Neuropathol* 2010;119:291–302
- Guidoux C, Hauw JJ, Klein IF, et al. Amyloid angiopathy in brain hemorrhage: A postmortem neuropathological-magnetic resonance imaging study. *Cerebrovasc Dis* 2018;45:124–31
- Wagner KR, Sharp FR, Ardizzone TD, et al. Heme and iron metabolism: Role in cerebral hemorrhage. *J Cereb Blood Flow Metab* 2003;23:629–52
- Strassmann G. Hemosiderin and tissue iron in the brain, its relationship, occurrence and importance; a study on 93 human brains. *J Neuropathol Exp Neurol* 1945;4:393–401
- Koeppen AH, Dickson AC, McEvoy JA. The cellular reactions to experimental intracerebral hemorrhage. *J Neurol Sci* 1995;134:102–12
- Oehmichen M, Raff G. Timing of cortical contusion. Correlation between histomorphologic alterations and post-traumatic interval. *Z Rechtsmed* 1980;84:79–94
- Oehmichen M, Eisenmenger W, Raff G, et al. Brain macrophages in human cortical contusions as indicator of survival period. *Forensic Sci Int* 1986;30:281–301

36. Vanezis P. Interpreting bruises at necropsy. *J Clin Pathol* 2001;54:348–55
37. Meguro R, Asano Y, Odagiri S, et al. Nonheme-iron histochemistry for light and electron microscopy: A historical, theoretical and technical review. *Arch Histol Cytol* 2007;70:1–19
38. Iancu TC. Ultrastructural aspects of iron storage, transport and metabolism. *J Neural Transm (Vienna)* 2011;118:329–35
39. Koeppe AH. The history of iron in the brain. *J Neurol Sci* 1995;134:1–9
40. Parmley RT, Spicer SS, Alvarez CJ. Ultrastructural localization of nonheme cellular iron with ferrocyanide. *J Histochem Cytochem* 1978;26:729–41
41. Brenner DS, Drachenberg CB, Papadimitriou JC. Structural similarities between hematoidin crystals and asteroid bodies: Evidence of lipid composition. *Exp Mol Pathol* 2001;70:37–42
42. Brandner S. *Histopathology of cerebral microbleeds*. In: Werring DJ, ed. *Cerebral Microbleeds Pathophysiology to Clinical Practice*. Cambridge, UK: Cambridge University Press; 2011:49–64
43. Hase Y, Chen A, Bates LL, et al. Severe white matter astrocytopathy in CADASIL. *Brain Pathol* 2018;28:832–43
44. Yamamoto Y, Hase Y, Ihara M, et al. Neuronal densities and vascular pathology in the hippocampal formation in CADASIL. *Neurobiol Aging* 2021;97:33–40
45. Skrobot OA, Attems J, Esiri M, et al. Vascular cognitive impairment neuropathology guidelines (VCING): The contribution of cerebrovascular pathology to cognitive impairment. *Brain* 2016;139:2957–69
46. Deramecourt V, Slade JY, Oakley AE, et al. Staging and natural history of cerebrovascular pathology in dementia. *Neurology* 2012;78:1043–50
47. Blevins BL, Vinters HV, Love S, et al. Brain arteriolosclerosis. *Acta Neuropathol* 2021;141:1–24
48. Craggs LJJ, Yamamoto Y, Deramecourt V, et al. Microvascular pathology and morphometrics of sporadic and hereditary small vessel diseases of the brain. *Brain Pathol* 2014;24:495–509
49. Soontornniyomkij V, Lynch MD, Mermash S, et al. Cerebral microinfarcts associated with severe cerebral beta-amyloid angiopathy. *Brain Pathol* 2010;20:459–67
50. Dallaire-Théroux C, Saikali S, Richer M, et al. Histopathological analysis of cerebrovascular lesions associated with aging. *J Neuropathol Exp Neurol* 2022;81:97–105
51. Dwork AJ, Schon EA, Herbert J. Nonidentical distribution of transferrin and ferric iron in human brain. *Neuroscience* 1988;27:333–45
52. Janaway BM, Simpson JE, Hoggard N, et al.; MRC Cognitive Function and Ageing Neuropathology Study. Brain haemosiderin in older people: Pathological evidence for an ischaemic origin of magnetic resonance imaging (MRI) microbleeds. *Neuropathol Appl Neurobiol* 2014;40:258–69
53. Cervos-Navarro J, Ulrich H. *Disorders of mineral metabolism. In: Metabolic and Degenerative Diseases of the Central Nervous System: Pathology, Biochemistry, and Genetics*. San Diego, CA: Academic Press; 1995:401–26
54. Davis PR, Giannini G, Rudolph K, et al. $A\beta$ vaccination in combination with behavioral enrichment in aged beagles: Effects on cognition, $A\beta$, and microhemorrhages. *Neurobiol Aging* 2017;49:86–99
55. Fisher M, French S, Ji P, et al. Cerebral microbleeds in the elderly: A pathological analysis. *Stroke* 2010;41:2782–5
56. Rajani RM, Ratelade J, Domenga-Denier V, et al. Blood brain barrier leakage is not a consistent feature of white matter lesions in CADASIL. *Acta Neuropathol Commun* 2019;7:187
57. Uchida Y, Kan H, Sakurai K, et al. Iron leakage owing to blood-brain barrier disruption in small vessel disease CADASIL. *Neurology* 2020;95:e1188–98
58. Craggs LJJ, Fenwick R, Oakley AE, et al. Immunolocalization of platelet-derived growth factor receptor- β (PDGFR- β) and pericytes in cerebral autosomal dominant arteriopathy with subcortical infarcts and leukoencephalopathy (CADASIL). *Neuropathol Appl Neurobiol* 2015;41:557–70
59. Wadi LC, Grigoryan MM, Kim RC, et al. Mechanisms of cerebral microbleeds. *J Neuropathol Exp Neurol* 2020;42:1093–9
60. Sumbria RK, Grigoryan MM, Vasilevko V, et al. A murine model of inflammation-induced cerebral microbleeds. *J Neuroinflammation* 2016;13:218
61. Ghosh M, Balbi M, Hellal F, et al. Pericytes are involved in the pathogenesis of cerebral autosomal dominant arteriopathy with subcortical infarcts and leukoencephalopathy. *Ann Neurol* 2015;78:887–900
62. Ruchoux MM, Kalaria RN, Román GC. The pericyte: A critical cell in the pathogenesis of CADASIL. *Cereb Circ Cogn Behav* 2021;2:100031
63. Kövari E, Charidimou A, Herrmann FR, et al. No neuropathological evidence for a direct topographical relation between microbleeds and cerebral amyloid angiopathy. *Acta Neuropathol Commun* 2015;3:49
64. Connor JR, Menzies SL, Martin SMS, et al. Cellular distribution of transferrin, ferritin, and iron in normal and aged human brains. *J Neurosci Res* 1990;27:595–611
65. Ward RJ, Zucca FA, Duyn JH, et al. The role of iron in brain ageing and neurodegenerative disorders. *Lancet Neurol* 2014;13:1045–60
66. Lassmann H. Hypoxia-like tissue injury as a component of multiple sclerosis lesions. *J Neurol Sci* 2003;206:187–91
67. Gerales R, Esiri MM, DeLuca GC, et al. Age-related small vessel disease: A potential contributor to neurodegeneration in multiple sclerosis. *Brain Pathol* 2017;27:707–22
68. Back SA, Luo NL, Borenstein NS, et al. Late oligodendrocyte progenitors coincide with the developmental window of vulnerability for human perinatal white matter injury. *J Neurosci* 2001;21:1302–12
69. Amberla K, Wäljas M, Tuominen S, et al. Insidious cognitive decline in CADASIL. *Stroke* 2004;35:1598–602
70. Tuominen S, Miao Q, Kurki T, et al. Positron emission tomography examination of cerebral blood flow and glucose metabolism in young CADASIL patients. *Stroke* 2004;35:1063–7
71. Craggs LJJ, Yamamoto Y, Ihara M, et al. White matter pathology and disconnection in the frontal lobe in cerebral autosomal dominant arteriopathy with subcortical infarcts and leukoencephalopathy (CADASIL). *Neuropathol Appl Neurobiol* 2014;40:591–602
72. Guindi M. Liver disease in iron overload. In: Saxena R, ed. *Practical Hepatic Pathology: A Diagnostic Approach*. Philadelphia, PA: Elsevier; 2018:151–65
73. Sun C, Wu Y, Ling C, et al. Deep gray matter iron deposition and its relationship to clinical features in cerebral autosomal dominant arteriopathy with subcortical infarcts and leukoencephalopathy patients: A 7.0-T magnetic resonance imaging study. *Stroke* 2020;51:1750–7
74. Liem MK, Oberstein SAJL, Versluis MJ, et al. 7 T MRI reveals diffuse iron deposition in putamen and caudate nucleus in CADASIL. *J Neurol Neurosurg Psychiatry* 2012;83:1180–5
75. De Reuck J, Auger F, Cordonnier C, et al. Comparison of 7.0-T T2-magnetic resonance imaging of cerebral bleeds in post-mortem brain sections of Alzheimer patients with their neuropathological correlates. *Cerebrovasc Dis* 2011;31:511–7
76. Strassmann G. Iron and calcium deposits in the brain; their pathological significance. *J Neuropathol Exp Neurol* 1949;8:425–35
77. Casanova MF, Araque JM. Mineralization of the basal ganglia: Implications for neuropsychiatry, pathology and neuroimaging. *Psychiatry Res* 2003;121:59–87
78. Hurst EW. On the so-called calcification in the basal ganglia of the brain. *J Pathol* 1926;29:65–85
79. Slager UT, Wagner JA. The incidence, composition, and pathological significance of intracerebral vascular deposits in the basal ganglia. *J Neuropathol Exp Neurol* 1956;15:417–31
80. Viswanathan A, Guichard JP, Gschwendner A, et al. Blood pressure and haemoglobin A1c are associated with microhae-

- morrhage in CADASIL: A two-centre cohort study. *Brain* 2006;129:2375–83
81. Nannucci S, Rinnoci V, Pracucci G, et al. Location, number and factors associated with cerebral microbleeds in an Italian-British cohort of CADASIL patients. *PLoS One* 2018;13:e0190878
82. Lee JS, Ko KH, Oh JH, et al. Cerebral microbleeds, hypertension, and intracerebral hemorrhage in cerebral autosomal-dominant arteriopathy with subcortical infarcts and leukoencephalopathy. *Front Neurol* 2017;8:203
83. Van Den Boom R, Lesnik Oberstein SAJ, Ferrari MD, et al. Cerebral autosomal dominant arteriopathy with subcortical infarcts and leukoencephalopathy: MR imaging findings at different ages—3rd–6th decades. *Radiology* 2003;229:683–90
84. Fazekas F, Kleinert R, Roob G, et al. Histopathologic analysis of foci of signal loss on gradient-echo T2-weighted MR images in patients with spontaneous intracerebral hemorrhage: Evidence of microangiopathy-related microbleeds. *AJNR Am J Neuroradiol* 1999;20:637–42
85. De Reuck J, Deramecourt V, Cordonnier C, et al. Prevalence of small cerebral bleeds in patients with a neurodegenerative dementia: A neuropathological study. *J Neurol Sci* 2011;300:63–6